

Two-dimensional electron honey: highly viscous electron fluid in which transverse magnetosonic waves can propagate

P. S. Alekseev and A. P. Alekseeva
Ioffe Institute, 194021 St. Petersburg, Russia

One of the main macroscopic differences between ordinary and highly viscous fluids is the lack of transverse sound in the first and possibility of its excitation in the second. In modern high-mobility conductors (Weyl semimetals, best-quality quantum wells, and graphene) electrons can form a viscous fluid at low temperatures. In this work we develop high-frequency hydrodynamics of two-dimensional highly viscous electron fluids in magnetic field. Such fluids are characterized by simultaneous presence of the excitations associated with the elastic stress (transverse sound) as well as with the violation of the local charge neutrality (plasmons). We demonstrate that both the viscoelastic and the plasmonic components of a flow can exhibit the *viscous resonance* that was recently proposed for charged viscous fluids. This resonance is related to rotation of the viscous stress tensor of a charged fluid in magnetic field. We argue that the viscous resonance is responsible for the peak and the peculiarities observed in photoresistance and photovoltage of the ultra-high mobility GaAs quantum wells. We conclude that a highly viscous electron fluid (“electron honey”) is realized in those structures.

PACS numbers: 72.80.Vp, 73.21.Fg, 72.20.-i, 72.15.Nj, 72.30.+q

1. Introduction. In materials with enough weak disorder phonons and conduction electrons can form viscous fluids provided that the inter-particle collisions conserving momentum are much more intensive than any other collisions which do not conserve momentum [1]. The hydrodynamic regime of phonon transport in liquid helium and dielectrics was studied several decades ago in sufficient details [2, 3]. However, only recently the hydrodynamic regime of charge transport was discovered in the novel ultra-high quality materials: GaAs quantum wells [4–9], 2D monovalent layered metal PdCoO₂ [10], 3D Weyl semimetal WP₂ [11], and graphene [12–14]. These experimental discoveries were accompanied by an extensive development of theory [15–36].

One of the evidences of the hydrodynamic regime of electron transport is the giant negative magnetoresistance effect, which is the decrease of resistance by 1-2 orders of magnitude in moderate magnetic fields, was discovered in the best-quality GaAs quantum wells [4–7], the Weyl semimetal WP₂ [11], and, very recently, in graphene [14]. This effect was explained by the hydrodynamic model taking into account the dependence of the viscosity coefficients of electrons on magnetic field and temperature [19]. Another evidence of forming a viscous electron fluid in graphene and high-mobility GaAs quantum wells is observation of the negative nonlocal resistance related to formation of whirlpools [9, 12, 20].

High-frequency transport in a viscous electron fluid was theoretically considered in several recent publications [30–33]. An ac flow of the fluid in a long sample in zero magnetic field was studied in Refs. [30, 31]. A Navier-Stokes equation for the two-dimension (2D) electron fluid in magnetic field with taking into account the time dispersion of viscosity was derived in Refs. [24, 33]. The ac viscosity coefficients of 2D electrons have a res-

onance at a frequency ω equal to the doubled electron cyclotron frequency $2\omega_c$ [33]. Such the *viscous resonance* manifests itself in the damping coefficient of magneto-plasmons [33]. Plasmons and transverse zero sound in a 2D electron Fermi liquid in zero magnetic field were studied in Refs. [34, 36]

In this work we demonstrate that the viscous resonance can be used to detect the excitation of transverse zero sound in a highly viscous electron fluid. We provide the evidences that this phenomenon have been observed in recent experiments on the 2D electron fluid in the best-quality GaAs quantum wells [37–39].

An ac flow of a highly viscous electron fluid in a microwave electric field consists of the plasmonic part formed by standing waves of plasmons and the viscoelastic part formed by standing waves of transverse zero sound. The last exists in Fermi liquids with enough strong interaction between quasi-particles [40]. We study transverse zero sound in a 2D electron Fermi liquid in magnetic field. We use the hydrodynamic approximation, which is valid at strong enough inter-particle interaction. The viscoelastic contribution determine the flow in the near-edge regions of wide samples and in the whole space in narrow samples [30, 31]. We demonstrate that in a perpendicular magnetic field the standing waves of the transverse zero sound are formed at the frequencies above the viscous resonance frequency, $\omega > 2\omega_c$, and are not formed at $\omega < 2\omega_c$. Because of this change of the flow, an ac current in narrow samples exhibits the viscous resonance at $\omega = 2\omega_c$. Around these frequencies the behavior of the electron fluid resembles one of an amorphous elastic media near the viscoelasticity transition, so the term “electron honey” can be coined.

We discuss the giant peak and the peculiarities that were recently observed in photoresistance and photovolt-

age of ultra-high mobility GaAs quantum wells at the frequencies near $\omega = 2\omega_c$ [37–39]. We argue that excitation of transverse zero sound, leading to the viscous resonance, is responsible for the observed phenomena. We also discuss that the independence of the viscoelastic part of the flow on the sign of the circular polarization of radiation correlates with the experiments [41–44]. We believe that the phenomena studied in this work should be expected in high-quality graphene and other material where the viscous transport have been recently realized.

2. *Ac hydrodynamics of 2D electron Fermi gas and strongly non-ideal Fermi liquid.* If the inter-particle interaction of electrons is weak and they can be regarded as an almost ideal Fermi gas, the hydrodynamic approach can be used when the characteristic space scale W of changing of the hydrodynamic velocity $\mathbf{V}(\mathbf{r}, t)$ is far greater than, at least, one of the following lengths: the electron mean free path relative to electron-electron collisions $l_{ee} = v_F \tau_{ee}$; the electron cyclotron radius $R_c = v_F / \omega_c$; the length of the path that free electron passes during the period of changing of $\mathbf{V}(\mathbf{r}, t)$, $l_\omega = v_F / \omega$ [1]. Here $\mathbf{r} = (x, y)$ is the coordinate in the 2D layer, v_F is the Fermi velocity, ω is a characteristic frequency of a flow, ω_c is the cyclotron frequency, and τ_{ee} is the electron-electron scattering time.

An ac flow of the electron gas is described by the particle density $n(\mathbf{r}, t) = n_0 + \delta n(\mathbf{r}, t)$ and the hydrodynamic velocity $\mathbf{V}(\mathbf{r}, t)$ (n_0 is the equilibrium density). We decompose $\delta n(\mathbf{r}, t)$ and $\mathbf{V}(\mathbf{r}, t)$ by time harmonics proportional to $e^{-i\omega t}$ with the complex amplitudes $\delta n(\mathbf{r})$ and $\mathbf{V}(\mathbf{r})$. In the regime linear by the external ac electric field, the continuity equation and the Navier-Stokes equation in magnetic field $\mathbf{B} = B\mathbf{e}_z$ at the frequencies ω compared with ω_c and $1/\tau_{ee}$ have the form [33, 45]:

$$-i\omega \delta n + n_0 \operatorname{div} \mathbf{V} = 0, \quad (1)$$

$$-i\omega \mathbf{V} = e\mathbf{E}/m + \omega_c \mathbf{V} \times \mathbf{e}_z + \eta_{xx} \Delta \mathbf{V} + \eta_{xy} \Delta \mathbf{V} \times \mathbf{e}_z, \quad (2)$$

where $\mathbf{E} = \mathbf{E}(\mathbf{r})$ is the complex amplitude of the electric field $\mathbf{E}(\mathbf{r}, t)$, e is the electron charge, m is the electron mass, and the ac viscosity coefficients $\eta_{xx} = \eta_{xx}(\omega)$ and $\eta_{xy} = \eta_{xy}(\omega)$ have the form [33]:

$$\left. \begin{array}{l} \eta_{xx} \\ \eta_{xy} \end{array} \right\} = \frac{\eta_0}{1 + (-\omega^2 + 4\omega_c^2)\tau_{ee}^2 - 2i\omega\tau_{ee}} \left\{ \begin{array}{l} 1 - i\omega\tau_{ee} \\ 2\omega_c\tau_{ee} \end{array} \right., \quad (3)$$

Here $\eta_0 = v_F^2 \tau_{ee} / 4$ is the viscosity in zero magnetic field.

In Eq. (2) we omit the hydrodynamic pressure term, $-\nabla P/m$, and the bulk momentum relaxation term, $-\gamma \mathbf{V}$. Although a perturbation of the electron density $\delta n(\mathbf{r}, t)$ leads to a perturbation of pressure $\delta P(\mathbf{r}, t)$ as well as to arising of the electric field $\mathbf{E}_{int}(\mathbf{r}, t)$ due to violation of local charge neutrality, the value of $\nabla \delta P$ is much smaller than $e\mathbf{E}_{int}$ [45]. For weak enough disorder and low temperature, the bulk momentum relaxation

term, $-\gamma \mathbf{V}$ is important only in the very vicinity of the cyclotron resonance or in the central part of very wide samples [45].

At $\omega, \omega_c \gg 1/\tau_{ee}$ the viscosity coefficients (3) have a resonance at $\omega = 2\omega_c$. The origin of such *the viscous resonance* is rotation of the viscous stress tensor $\sigma'_{ij} = -m\langle v_i v_j \rangle$ in magnetic field with its own frequency $2\omega_c$ (\mathbf{v} is the velocity of a single electron and the triangular brackets denotes averaging by all electrons).

If the interaction between 2D electrons is strong, they must be treated as a Fermi liquid. Eqs. (1) and (2), describing in this case a fluid consisting of the quasiparticles of the Fermi liquid, can be derived from the kinetic equation for quasiparticles [52]. Herewith the coefficients n_0 and η_0 will contain not only the characteristics of the quasiparticle spectrum, but also the large Landau parameters, characterizing the interaction between quasiparticles [52]. Eigenmodes of a Fermi liquid allow hydrodynamic consideration within Eqs. (1) and (2) provided the following condition: the Landau parameters in the Fermi liquid units must be much greater than unity [53]. In this case, the value of the viscosity coefficient η_0 is mainly proportional to the Landau parameters, thus the parameter $v_F = 2\sqrt{\eta_0/\tau_{ee}}$ is much larger than the actual quasi-particle velocity at the Fermi sphere, v_{F0} : $v_F \gg v_{F0}$.

The electric field $\mathbf{E}(\mathbf{r}, t)$ consists of the two parts: the field of incident radiation $\mathbf{E}_0(t)$ and the internal field $\mathbf{E}_{int}(\mathbf{r}, t)$ induced by the perturbation of the electron density $\delta n(\mathbf{r}, t)$. We do not consider the retardation effects which can be important in the region of small wavevectors in some structures (see Ref. [54, 55]). Thus we use the electrostatic formula $\mathbf{E}_{int} = -\nabla \delta \varphi$. For the structures with a metallic gate located at the distance d from the 2D layer the electrostatic potential is: $\delta \varphi = (4\pi e d / \kappa) \delta n$, where κ is the background dielectric constant. For the structures without a gate the relation between $\delta \varphi(\mathbf{r}, t)$ and $\delta n(\mathbf{r}, t)$ is given by the Coulomb law with the 2D charge density $e \delta n$.

3. *Formation of the linear response.* There are the two types of waves that can be excited in a highly viscous electron fluid: magnetoplasmons and transverse zero magnetosound, the waves similar to the transverse sound in elastic media.

The magnetoplasmon waves are described by the one of the two wave solutions of Eqs. (1) and (2) in the absence of external ac field, $\mathbf{E}_0 = 0$. Neglecting the relaxation processes, we obtain the dispersion law of magnetoplasmons: $\omega_p(q) = \sqrt{\omega_c^2 + s^2 q^2}$, where $s = 2\sqrt{\pi e^2 n_0 d / m \kappa}$ is the plasmon velocity which is considered to be much greater than v_F . Damping coefficient of magnetoplasmons due to viscosity is [33]:

$$\Upsilon_p(q) = \frac{\omega_c^2 + \omega_p^2}{2\omega_p^2} q^2 \operatorname{Re} \eta_{xx} + \frac{\omega_c}{\omega_p} q^2 \operatorname{Im} \eta_{xy}. \quad (4)$$

Here the viscosity coefficients $\eta_{xx} = \eta_{xx}(\omega)$ and $\eta_{xy} =$

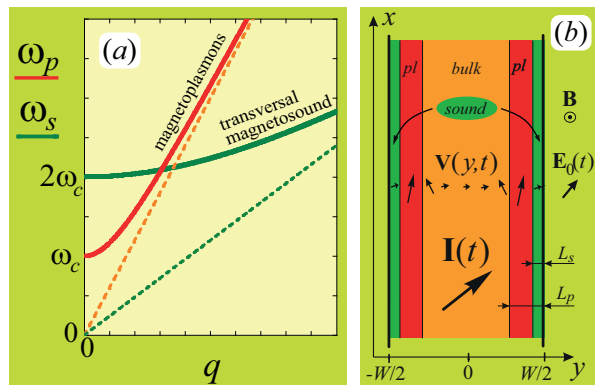


FIG. 1: (a) The dispersion laws of magnetoplasmons and transverse zero sound. The dashed lines demonstrates the dispersion laws in zero magnetic field. At $q \rightarrow 0$ the viscosity stress tensor of the fluid rotates with the frequency $\omega_s(0) = 2\omega_c$. (b) A long sample in circularly polarized ac electric field $\mathbf{E}_0(t)$ and perpendicular magnetic field \mathbf{B} . The sample width W is larger than the decay lengths L_p and L_s of magnetoplasmons and magnetosound, thus the three types of regions are formed: the central region where the flow is controlled by the bulk momentum relaxation; the near-edge layers with the widths L_s in which the flow is governed by viscosity; and the regions $L_s < |y - W/2| < L_p$ where the flow is formed magnetoplasmons.

$\eta_{xy}(\omega)$ are taken at $\omega = \omega_p(q)$. Damping of magnetoplasmons due to scattering on disorder in high-quality samples with very small γ is important only in the very vicinity of the cyclotron resonance, $|\omega - \omega_c| \lesssim \gamma$ [45].

The second wave solution of Eqs. (1) and (2) at $\mathbf{E}_0 = 0$ corresponds to magnetosound, whose amplitude \mathbf{V}_0 is perpendicular to the wavevector \mathbf{q} . Such transverse sound is related to an elastic part of the shear stress, which arises in an inhomogeneous ac flow of a viscous fluid. Within the hydrodynamic approximation, the magnetosound dispersion law $\omega_s(q)$ and its damping coefficient $\Upsilon_s(q)$ come from the time dispersion of viscosity (3). At high frequencies, $\omega_c, \omega \gg 1/\tau_{ee}$, one obtains [45]:

$$\omega_s(q) = \sqrt{4\omega_c^2 + \frac{v_F^2 q^2}{4}}, \quad \Upsilon_s(q) = \frac{4\omega_c^2 + \omega_s^2}{2\omega_s^2 \tau_{ee}}. \quad (5)$$

As it was discussed above, for a strongly non-ideal Fermi liquid the parameter v_F is much greater than the actual Fermi velocity v_{F0} . Therefore the magnetosound wavelength, having the order of magnitude $l_s = l_\omega = v_F/\omega$ at $\omega_c \sim \omega$, is much larger than the path that a quasiparticle passes during one period of ac field, $\sim v_{F0}/\omega$. Thus we can consider the flows with the character spacescales W as small as $v_{F0}/\omega \ll W \ll l_\omega$. For our case $s \gg v_F$ the dispersions laws $\omega_p(q)$ and $\omega_s(q)$ are shown at Fig. 1(a).

Next, we calculate a linear response of the fluid on a

circularly polarized ac electric field $\mathbf{E}_0(t) = \mathbf{E}_0 e^{-i\omega t} + c.c.$, where $E_{0,x} = E_0/2$, $E_{0,y} = \mp i E_0/2$, and the signs “-” and “+” correspond to the right and the left circular polarizations. We consider only the structures with a gate, believing that the main results will be quantitatively the same for ungated structures, while the calculations will be far more complex.

We study a flow in a long sample with rough boundaries, at which the zero boundary conditions, $\mathbf{V}(y = \pm W/2) = 0$, are fulfilled. Herewith the layers formed by the magnetoplasmons and magnetosound are separated in space and have the widths L_p and L_s of different orders of magnitudes (see Fig. 1(b) and Ref. [45]). The result for the complex amplitude $I = en_0 \int_{-W/2}^{W/2} \mathbf{V}(y) dy$ of the current $\mathbf{I}(t)$ in the main order by the parameter $v_F/s \ll 1$ is [45, 56]:

$$\frac{\mathbf{I}}{I_0} = \frac{\omega}{\tilde{\omega} - \omega_c} \begin{pmatrix} i \\ \pm 1 \end{pmatrix} \pm \frac{f_p}{\tilde{\omega} - \omega_c} \begin{pmatrix} i\omega_c \\ -\omega \end{pmatrix} - i \frac{f_s}{\omega} \begin{pmatrix} 1 \\ 0 \end{pmatrix}, \quad (6)$$

where $I_0 = e^2 n_0 E_0 W / (2m\omega)$; the first term is the usual Drude contribution, which dominates in the central part of wide samples; $\tilde{\omega} = \omega + i\gamma$ takes into account a weak scattering on disorder; the second and the third terms, being proportional to $f_{p,s} = \tanh(\lambda_{p,s}W/2)/(\lambda_{p,s}W/2)$, describe the plasmonic and the viscoelastic contributions, respectively; $\lambda_p = iq_p - \omega\Upsilon_p/(s^2q_p)$ corresponds to the magnetoplasmons with the decay length $L_p = |1/\text{Re}\lambda_p|$, $q_p = \sqrt{\omega^2 - \omega_c^2}/s$ is the magnetoplasmon wavevector; and $\lambda_s = -i\omega/\eta_{xx}$ corresponds to the magnetosound with the decay length $L_s = |1/\text{Re}\lambda_s|$.

It is noteworthy that the viscoelastic part of the current (6) is independent on the sign of the circular polarization.

4. *Properties of the linear response.* The linear response (6) describes, in particular, absorption of energy from ac field. The dependance of the absorption power $\mathcal{W} = 2\text{Re}(\mathbf{E}_0^* \mathbf{I})$ on ω and ω_c changes its character with changing the sample width and exhibits the resonances related to the Drude, the plasmonic and the viscoelastic parts of the ac flow.

In very wide samples, $W \gg L_p$, absorption is mainly determined by the Drude part of the flow in the central part of the sample [see Fig. 1(b)]. The function $\mathcal{W}(\omega_c)$ for a fixed ω exhibit the cyclotron resonance at $\omega_c = \omega$.

In moderately wide samples, $l_p \ll W \ll L_p$, the standing waves of magnetoplasmons are formed inside the whole sample at ac frequencies above the cyclotron resonance, $\omega > \omega_c$. Here $l_p = s/\omega$ is the characteristic magnetoplasmon wavelength at $\omega \sim \omega_c$. When the sample width is equal to an integer or a half-integer number of magnetoplasmon wavelengths, $W = m\pi/q_p(\omega_c)$ (m is an integer, ω is fixed), $\mathcal{W}(\omega_c)$ exhibits the plasmonic resonances [see Fig. 2(a)]. The plasmonic resonance frequency $\omega_{c,p}(W)$ can fall in the vicinity of the viscous resonance, $\omega_c = \omega/2$, or away from it. Herewith the

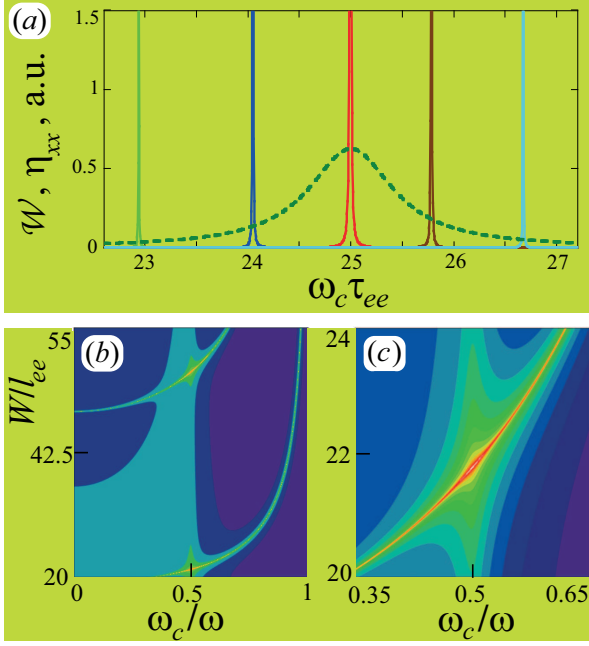


FIG. 2: (a) Absorption power \mathcal{W} as a function of ω_c at fixed ω for the wide samples ($W/l_{ee} = 148.5, 150.5, 152.35, 154, 156$ for green, blue, red, brown, and light-blue solid curves) at $\omega\tau_{ee} = 50$ and $s/v_F = 300$. The dependencies $\mathcal{W}(\omega_c)$ exhibit the plasmonic resonances, whose frequencies $\omega_{c,p}$ depend on the sample width W . Dashed line is the dissipative parts of the viscosity coefficients, $\text{Re}\eta_{xx} = \text{Im}\eta_{xy}$. The width of plasmonic resonances is maximal at the maximum of $\text{Re}\eta_{xx}(\omega_c)$. (b,c) Colormaps of the function $\mathcal{W}(\omega_c, W)$. Maximums of \mathcal{W} , are located at the intersections of the region $\omega_c \approx \omega/2$ attributed the viscous resonance by the bent narrow regions attributed the plasmonic resonances.

width of the plasmonic resonance, which is proportional to the damping coefficient due to viscosity (4), resonantly depends on $\omega_c - \omega/2$ (see Fig. 2).

In medium samples, $L_s \ll W \ll l_p$, at ac frequencies above the viscous resonance, $\omega > 2\omega_c$ the flow in the near-edge regions, $W/2 - |y| \lesssim L_s$, have the form of the standing waves of the transverse zero sound. Below the viscous resonance, $\omega < 2\omega_c$, the viscous part of the flow is located in the narrower near-edge layers, $W/2 - |y| \lesssim l_s$ ($l_s \ll L_s$, and has an exponential non-oscillating profile. Due to such change of the type of the flow near $\omega = 2\omega_c$, the viscous resonance arises as an asymmetric peak in the dependencies $\mathcal{W}(\omega_c)$ and $\mathbf{I}(\omega_c)$ [see Fig. 3(a,b)]. From Eq. (6) one obtains near the resonance [45]:

$$\mathcal{W}(\omega_c) \propto \text{Re}[-i + (2\omega_c - \omega)\tau_{ee}]^{-1/2}. \quad (7)$$

Such peak is strongly asymmetric relative to the point $\omega_c = \omega/2$ [see Fig. 3(a,b)].

In narrow samples, $l_s \ll W \ll L_s$, standing waves of magnetosound are formed in the whole sample at $\omega > 2\omega_c$. When the sample width becomes equal to an integer or a half-integer number of magnetosound wavelengths,

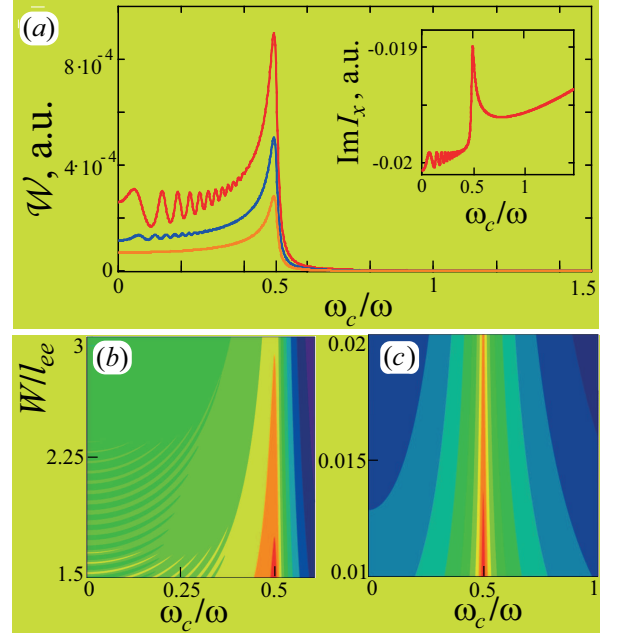


FIG. 3: (a) Absorption power \mathcal{W} as a function of ω_c at fixed ω for medium and narrow samples widths $W/l_{ee} = 5.7, 3.2, 1.8$ (yellow, blue, and red curves) at $\omega\tau_{ee} = 50$ and $s/v_F = 300$. Inset presents the imaginary part of the ac current $I_x(\omega_c)$ for a medium sample ($W/l_{ee} = 1.8$). The viscous resonance at $\omega_c = \omega/2$ and the magnetosound resonances $\omega_{c,s} = \omega_{c,s}(m)$ are seen. (b,c) Colormaps of the functions $\mathcal{W}(\omega_c, W)$ and $R(\omega_c, W)$ for medium and very narrow samples, respectively. The profile of the viscous resonance is asymmetric for medium and narrow samples and symmetric for very narrow samples.

$W = m\pi/q_s(\omega_c)$, the resonances $\omega_{c,s} = \omega_{c,s}(m)$ related to standing magnetosound waves appear in $\mathcal{W}(\omega_c)$ ($q_s = 2\sqrt{\omega^2 - 4\omega_c^2}/v_F$ is the magnetosound wavevector). Such resonances, shown at Figs. 2(a,b), can be named the “magnetosound resonances”.

In maximally narrow samples, $W \ll l_s$, the velocity $\mathbf{V}(y)$ has a parabolic profile in a whole sample [45]. This regime can be regarded as the ac Poiseuille flow in magnetic field. The viscous resonance manifests itself not in the current, but in the ac impedance $Z = E/I_x$. Near the resonance Eq. (6) for the real part of the impedance $R = \text{Re}Z$ yields:

$$R(\omega_c) \propto [1 + (2\omega_c - \omega)^2\tau_{ee}^2]^{-1}. \quad (8)$$

This is the Lorenz profile, symmetric relative to the point $\omega_c = \omega/2$ [see Fig. 3(c)]. At $\omega\tau_{ee} \gg 1$ the imaginary part of the current (6), $\text{Im}I_x = I_0(4\omega_c^2 - \omega^2)W^2/(3v_F^2)$, does not depend on any relaxation parameter. Such result corresponds to ac field-induced oscillations of a charged elastic 2D media, glued to the edges $y = \pm W/2$. The inter-particle scattering with the rate τ_{ee} is responsible for damping of this oscillations.

We conclude that the viscoelasticity transition occurs in the system with decrease of the sample width W below

the magnetosound damping length L_s and increase of ac frequency ω above $1/\tau_{ee}$.

5. *Manifestation of the viscous resonance in non-linear effects.* In high-mobility GaAs quantum wells bright surprising effects were observed at the frequencies $\omega = 2\omega_c$ in non-linear ac magnetotransport: a strong peak in photoresistance [37, 38] and a peculiarity in the photovoltaic effect [39]. Below we present the arguments that the viscous resonance is responsible for these effects.

It was stressed in Ref. [37] that the strong peak in photoresistance and a very well pronounced giant negative magnetoresistance, explained in Ref. [19] as a manifestation of forming a viscous flow, are observed in the *same best-quality* GaAs structures. If 2D electrons in such structures form a viscous fluid, any ac effect must inevitably have peculiarities at the frequency of the viscous resonance.

We have demonstrated that the peak of the viscous resonance can be asymmetric as well as symmetric, depending on the sample width. Both these two forms of the peak were observed in photoconductivity in experiments [37, 38] at different conditions.

In Ref. [39] the photovoltage effect was measured on several GaAs quantum well structures of different geometries. The peculiarity at $\omega = 2\omega_c$ was much better observed in the sample having a meander-shaped gate, compared with the uniformly-gated and ungated samples. Apparently, the meander-shaped gate leads to inhomogeneous perturbations of the electron flow. Thus in the meander-gated sample the role of viscosity must be greater than in the other samples and the viscous resonance is expected to be more pronounced, as it was observed.

In Refs. [41–44] it was shown that photoresistance of high-mobility GaAs quantum wells is usually almost independent of the sign of circular polarization of radiation at $\omega_c \lesssim \omega$. Although the discussed above giant peak in photoresistance was observed up to now only for the linear polarization of ac field, a detailed analysis [45] of the results of Refs. [41–44] correlates with the statement that the peak has the hydrodynamic nature.

The assumption about the strong interaction between quasiparticles of the electron Fermi-liquid in the high-mobility GaAs quantum wells seems to be fulfilled. Indeed, the parameter r_s characterizing the strength of the Coulomb interaction in a 2D electron system is about unity for the structures studied in Refs. [37–39]. In addition, there are experimental evidences that the effective mass of 2D electrons in the high-mobility GaAs quantum wells is strongly renormalized due to the inter-particle interaction [57, 58]. Our preliminary analysis [53] demonstrates that the strong interaction between quasiparticles in the 2D electron Fermi liquid justify the applicability of hydrodynamics for the proper description of magnetosonic perturbations in such fluids.

6. *Acknowledgements.* The authors thank

M. I. Dyakonov for numerous illuminating discussions of transport phenomena in high-mobility two-dimensional electron systems which led to the current work, as well as for discussions of some of the issues raised in this work; I. V. Gornyi for kind interest, discussions, advice, and support, as well as for attracting authors' attention to some of the references; E. G. Alekseeva, I. P. Alekseeva, N. S. Averkiev, A. I. Chugunov, A. P. Dmitriev, M. M. Glazov, I. V. Krainov, A. N. Poddubny, P. S. Shternin, D. S. Svinin, V. A. Volkov, A. A. Zyuzin, and A. Yu. Zyuzin for valuable discussions, advice, and support; and D. G. Polyakov for reading the preprint of the manuscript and the critical remarks that helped to substantially improve it.

The part of this work devoted to calculation of the linear response of the viscous electron fluid (Section “Formation of the linear response”) was supported by the Russian Science Foundation (Grant No. 17-12-01182); the part of this work devoted to the study of the ways of manifestation of the viscous resonance in the viscous electron fluid (Section “Properties of the linear response”) was supported by the grant of the Basis Foundation (Grant No. 17-14-414-1); the part of this work devoted to analysis of applicability of the hydrodynamic model of strongly non-ideal electron fluid for real high-mobility GaAs quantum wells (Sections “Ac hydrodynamics of 2D electron Fermi gas and strongly non-ideal Fermi liquid” and “Manifestation of the viscous resonance in non-linear effects”) was supported by the Russian Science Foundation (Grant No. 18-72-10111).

-
- [1] R. N. Gurzhi, *Sov. Phys. Uspekhi* 94, 657 (1968).
 - [2] V. L. Gurevich, *Transport in Phonon Systems* (Elsevier Science Publishers, Amsterdam - New York, 1986).
 - [3] L. P. Pitaevskii, *Sov. Phys. Uspekhi* 11, 342 (1968).
 - [4] A. T. Hatke, M. A. Zudov, J. L. Reno, L. N. Pfeiffer, and K.W. West, *Phys. Rev. B* 85, 081304 (2012).
 - [5] R. G. Mani, A. Kriisa, and W. Wegscheider, *Scientific Reports* 3, 2747 (2013).
 - [6] L. Bockhorn, P. Barthold, D. Schuh, W. Wegscheider, and R. J. Haug, *Phys. Rev. B* 83, 113301 (2011).
 - [7] Q. Shi, P. D. Martin, Q. A. Ebner, M. A. Zudov, L. N. Pfeiffer, and K. W. West, *Phys. Rev. B* 89, 201301 (2014).
 - [8] G. M. Gusev, A. D. Levin, E. V. Levinson, and A. K. Bakarov, *AIP Advances* 8, 025318 (2018).
 - [9] A. D. Levin, G. M. Gusev, E. V. Levinson, Z. D. Kvon, and A. K. Bakarov, *Phys. Rev. B* 97, 245308 (2018).
 - [10] P. J. W. Moll, P. Kushwaha, N. Nandi, B. Schmidt, and A. P. Mackenzie, *Science* 351, 1061 (2016).
 - [11] J. Gooth, F. Menges, C. Shekhar, V. Suess, N. Kumar, Y. Sun, U. Drechsler, R. Zierold, C. Felser, and B. Gotsmann, arXiv:1706.05925 (2017).
 - [12] D. A. Bandurin, I. Torre, R. Krishna Kumar, M. Ben Shalom, A. Tomadin, A. Principi, G. H. Auton, E. Khestanova, K. S. Novoselov, I. V. Grigorieva, L. A. Ponomarenko, A. K. Geim, and M. Polini, *Science* 351, 1055

- (2016).
- [13] R. Krishna Kumar, D. A. Bandurin, F. M. D. Pellegrino, Y. Cao, A. Principi, H. Guo, G. H. Auton, M. Ben Shalom, L. A. Ponomarenko, G. Falkovich, K. Watanabe, T. Taniguchi, I. V. Grigorieva, L. S. Levitov, M. Polini, and A. K. Geim, *Nature Physics* 13, 1182 (2017).
- [14] A. I. Berdyugin, S. G. Xu, F. M. D. Pellegrino, R. Krishna Kumar, A. Principi, I. Torre, M. Ben Shalom, T. Taniguchi, K. Watanabe, I. V. Grigorieva, M. Polini, A. K. Geim, D. A. Bandurin, arXiv:1806.01606 (2018)
- [15] M. Hruska and B. Spivak, *Phys. Rev. B* 65, 033315 (2002).
- [16] A. V. Andreev, S. A. Kivelson, and B. Spivak, *Phys. Rev. Lett.* 106, 256804 (2011).
- [17] M. Mendoza, H. J. Herrmann, and S. Succi, *Scientific Reports* 3, 1052 (2013).
- [18] A. Tomadin, G. Vignale, and M. Polini, *Phys. Rev. Lett.* 113, 235901 (2014).
- [19] P. S. Alekseev, *Phys. Rev. Lett.* 117, 166601 (2016).
- [20] L. Levitov and G. Falkovich, *Nature Physics* 12, 672 (2016).
- [21] H. Guo, E. Ilseven, G. Falkovich, and L. Levitov, *PNAS* 114, 3068 (2017).
- [22] A. Lucas, *Phys. Rev. B* 95 115425 (2017).
- [23] A. Lucas and K.C. Fong, arXiv: 1710.08425 (2017).
- [24] F. M. D. Pellegrino, I. Torre, and M. Polini, *Phys. Rev. B* 96, 195401 (2017).
- [25] P. S. Alekseev, A. P. Dmitriev, I. V. Gornyi, V. Y. Kachorovskii, and M. A. Semina, *Semiconductors* 51, 766 (2017).
- [26] P. S. Alekseev, A. P. Dmitriev, I. V. Gornyi, V. Yu. Kachorovskii, B. N. Narozhny, and M. Titov, *Phys. Rev. B* 97, 085109 (2018).
- [27] P. S. Alekseev, A. P. Dmitriev, I. V. Gornyi, V. Yu. Kachorovskii, B. N. Narozhny, and M. Titov, *Phys. Rev. B* 98, 125111 (2018).
- [28] P. S. Alekseev and M. A. Semina, *Phys. Rev. B* 98, 165412 (2018).
- [29] O. Kashuba, B. Trauzettel, L. W. Molenkamp, *Phys. Rev. B* 97, 205129 (2018).
- [30] R. Moessner, P. Surowka, P. Witkowski, *Phys. Rev. B* 97, 161112 (2018).
- [31] M. Semenyakin and G. Falkovich, *Phys. Rev. B* 97, 085127 (2018).
- [32] R. Cohen and M. Goldstein, arXiv 1809.05847v1 (2018)
- [33] P. S. Alekseev, *Phys. Rev. B* 98, 165440 (2018).
- [34] A. Lucas and S. Das Sarma, *Phys. Rev. B* 97, 115449 (2018).
- [35] A. Lucas and S. Das Sarma, arXiv:1804.00665 (2018).
- [36] J. Y. Khoo and I. S. Villadiego, arXiv:1806.04157v2 (2018).
- [37] Y. Dai, R. R. Du, L. N. Pfeiffer, and K. W. West, *Phys. Rev. Lett.* 105, 246802 (2010).
- [38] A. T. Hatke, M. A. Zudov, L. N. Pfeiffer, and K. W. West, *Phys. Rev. B* 83, 121301 (2011).
- [39] M. Bialek, J. Lusakowski, M. Czapkiewicz, J. Wrobel, and V. Umansky, *Phys. Rev B* 91, 045437 (2015).
- [40] E. M. Lifshitz, L. P. Pitaevskii, *Statistical Physics, Part 2: Theory of the Condensed State. Vol. 9 (1st ed.)*. Pergamon Press (1981).
- [41] J. H. Smet, B. Gorshunov, C. Jiang, L. Pfeiffer, K. West, V. Umansky, M. Dressel, R. Meisels, F. Kuchar, and K. von Klitzing *Phys. Rev. Lett.* 95, 116804 (2007).
- [42] J.H. Smet, B. Gorshunov, C. Jiang, L. Pfeiffer, K. West, V. Umansky, M. Dressel, R. Meisels, F. Kuchar, K. von Klitzing, *Physica E* 35, 315 (2006).
- [43] T. Herrmann, I. A. Dmitriev, D. A. Kozlov, M. Schneider, B. Jentzsch, Z. D. Kvon, P. Olbrich, V. V. Belkov, A. Bayer, D. Schuh, D. Bougeard, T. Kuczmik, M. Oltcher, D. Weiss, and S. D. Ganichev *Phys. Rev. B* 94, 081301 (2016).
- [44] T. Herrmann, Z. D. Kvon, I. A. Dmitriev, D. A. Kozlov, B. Jentzsch, M. Schneider, L. Schell, V. V. Belkov, A. Bayer, D. Schuh, D. Bougeard, T. Kuczmik, M. Oltcher, D. Weiss, and S. D. Ganichev, *Phys. Rev. B* 96, 115449 (2017).
- [45] For details of calculations of the ac linear response and description of the flows in wide and narrow samples see Supplemental containing the refernces [46–51] (except the references that are mentioned in the main text).
- [46] M. B. Lifshits and M. I. Dyakonov, *Phys. Rev. B* 80, 121304 (2009).
- [47] Y. M. Beltukov and M. I. Dyakonov, *Phys. Rev. Lett.* 116, 176801 (2016).
- [48] I. A. Dmitriev, A. D. Mirlin, D. G. Polyakov, and M. A. Zudov, *Rev. Mod. Phys.* 84, 1709 (2012).
- [49] J. R. Dorfman and E. G. D. Cohen, *Phys. Lett.* 66, 124 (1965)
- [50] J. R. Dorfman and E. G. D. Cohen, *Phys. Rev. Lett.* 25, 1257 (1970).
- [51] A. Shytov, J. Feng Kong, G. Falkovich, and L. Levitov, *Phys. Rev. Lett.* 121, 176805 (2018).
- [52] I. M. Khalatnikov and A. A. Abrikosov, *Sov. Phys. JETP* 6, 84 (1958).
- [53] P. S. Alekseev and A. P. Alekseeva, to be published.
- [54] V. I. Fal'ko and D. E. Khmel'nitskii, *JETP* 68, 1150 (1989).
- [55] V. A. Volkov and A. A. Zabolotnykh, *Phys. Rev. B* 89, 121410 (2014).
- [56] For the case of zero magnetic field, the expression similar to Eqs. (24) and (25) were independently derived in Ref. [30, 31].
- [57] I. V. Kukushkin and V. A. Volkov, Two-dimensional electronic fluid in strong magnetic field, (Moscow, Fizmatkniga, 2016).
- [58] A. V. Shchepetilnikov, D. D. Frolov, Yu. A. Nefyodov, I. V. Kukushkin, and S. Schmult *Phys. Rev. B* 95, 161305 (2017).

Supplemental

1. Calculation of linear response of 2D electron fluid on ac electric field

In this section we present a calculation of the flow of a highly viscous 2D electron fluid in a long sample with rough boundaries.

In the regime linear by external ac electric field, the continuity and the Navier-Stokes equation for an electron fluid in magnetic field, taking into account bulk momentum relaxation, are [1]:

$$-i\omega \delta n + n_0 \text{div} \mathbf{V} = 0, \quad (9)$$

and

$$-i\omega \mathbf{V} = \frac{e}{m} \mathbf{E}(\mathbf{r}, \omega) + \omega_c [\mathbf{V} \times \mathbf{e}_z] - \gamma \mathbf{V} - \frac{\nabla P}{m} + \eta_{xx}(\omega) \Delta \mathbf{V} + \eta_{xy}(\omega) [\Delta \mathbf{V} \times \mathbf{e}_z], \quad (10)$$

where $\mathbf{E}(\mathbf{r}, \omega)$, $\delta n = \delta n(\mathbf{r}, \omega)$ and $\mathbf{V} = \mathbf{V}(\mathbf{r}, \omega)$ are the complex amplitudes of the harmonics of the electric field $\mathbf{E}(\mathbf{r}, t)$, the particle density $\delta n(\mathbf{r}, t)$, and the hydrodynamic velocity $\mathbf{V}(\mathbf{r}, t)$; n_0 is the unperturbed electron density; $e < 0$ is the electron charge; m is the electron mass; γ is the rate of momentum relaxation in bulk due to the electron scattering on disorder or phonons; P is the pressure in the electron gas; and the ac viscosity coefficients $\eta_{xx}(\omega)$ and $\eta_{xy}(\omega)$ depend on magnetic field and frequency as [1]:

$$\eta_{xx}(\omega) = \eta_0 \frac{1 - i\omega\tau_{ee}}{1 + (-\omega^2 + 4\omega_c^2)\tau_{ee}^2 - 2i\omega\tau_{ee}}, \quad (11)$$

$$\eta_{xy}(\omega) = \eta_0 \frac{2\omega_c\tau_{ee}}{1 + (-\omega^2 + 4\omega_c^2)\tau_{ee}^2 - 2i\omega\tau_{ee}}.$$

Here $\eta_0 = v_F^2 \tau_{ee} / 4$ is the 2D electron viscosity in the absence of magnetic field; τ_{ee} is the time of relaxation of the second harmonics (by the electron velocity angle) of the electron distribution function; and v_F is the Fermi velocity v_{F0} for the case of a weak electron-electron interaction and the parameter determined as $v_F = 2\sqrt{\eta/\tau_{ee}}$ for a strong inter-quasiparticle interaction. In the last case, v_F depends on the parameters of the Landau function describing the interaction of quasiparticles and is much greater than the Fermi velocity v_{F0} .

The electric field $\mathbf{E}(\mathbf{r}, t)$ consists of the two parts: external circularly polarized electric field $\mathbf{E}_0(t)$ and the internal electric field $\mathbf{E}_{int}(\mathbf{r}, t)$ induced by the perturbation of the 2D electron density $\delta n(\mathbf{r}, t)$. In this work we do not consider the retardation effects which can be important in the region of small wavevectors in some structures (see Ref. [2, 3]). When we can neglect the retardation effects, we just have the electrostatic formula $\mathbf{E}_{int} = -\nabla\delta\varphi$, where the electrostatic potential $\delta\varphi$ is related to δn . For

the structures with a metallic gate located at the distance d from the 2D layer we have:

$$\delta\varphi = \frac{4\pi ed}{\kappa} \delta n, \quad (12)$$

where κ is the background dielectric constant. For the structures without a gate the relation between $\delta\varphi(\mathbf{r}, t)$ and $\delta n(\mathbf{r}, t)$ is given just by the Coulomb law with the charge density $\varrho(\mathbf{r}, z, t) = e \delta n(\mathbf{r}, t) \delta(z)$, where $\delta(z)$ is the Delta-function depicting the position of the 2D layer:

$$\delta\varphi(\mathbf{r}, t) = e \int d^2\mathbf{r}' \frac{\delta n(\mathbf{r}', t)}{|\mathbf{r} - \mathbf{r}'|}. \quad (13)$$

The ratio of the terms $-\nabla P/m$ and $e\mathbf{E}_{int}/m$ in Eq. (10) is estimated as a_B/d for the structures with a gate and as $a_B q$ for the ungated structures, where a_B is the Bohr radius and q is the character wavevector. Both these values must be much smaller than unity when the 2D electrostatic equations are applicable.

Neglecting the relaxation processes and in the absence of the external electric field, $\mathbf{E}_0 = 0$, we obtain from Eqs. (9), (10), and (12) the usual formula for the dispersion law of magnetoplasmons. For the gated structures it is:

$$\omega_p(q) = \sqrt{\omega_c^2 + s^2 q^2}, \quad (14)$$

where $s = \sqrt{4\pi e^2 n_0 d / m\kappa}$. The second term under the square root, $s^2 q^2$, is the squared plasmon frequency in the absence of magnetic field. For the ungated structure it changes on $2\pi e^2 n_0 q / m\kappa$.

We calculate a linear response of the electron fluid on the circularly polarized homogeneous ac electric field $\mathbf{E}_0(t) = \mathbf{E}_0 e^{-i\omega t} + c.c.$,

$$\mathbf{E}_0 = \frac{E_0}{2} \begin{pmatrix} 1 \\ \mp i \end{pmatrix}, \quad (15)$$

where the signs “-” and “+” correspond to the right and the left circular polarizations of ac field.

We confine ourselves by consideration only the case of gated structures. We believe that the main physical results will be quantitatively the same for ungated structures, while the calculations will be far more complex for ungated structures due to non-local character of electrostatics in the ungated case [see Eq. (13)].

Let us consider a high-frequency flow in a long sample, $-L/2 \ll x \ll L/2$, $-W/2 \ll y \ll W/2$, $L \gg W$, with rough longitudinal boundaries. This is the simplest “minimal” model for studying viscous transport in the confined geometry. The velocity field $\mathbf{V}(\mathbf{r}, t)$ have the form: $\mathbf{V}(\mathbf{r}, t) = \mathbf{V}(y) e^{-i\omega t} + c.c.$, and the analogous formulas take place for $\delta n(\mathbf{r}, t)$ and $\delta U(\mathbf{r}, t)$. Substitution of $\delta n(y)$ and $\delta\varphi(y)$ from the continuity and the electrostatic equations (9) and (12) to the Navier-Stokes equation (10)

yields the closed equation for the complex amplitude of the velocity $\mathbf{V}(y)$:

$$\begin{pmatrix} i\tilde{\omega} + \eta \partial^2 & -(\omega_c + \bar{\eta} \partial^2) \\ \omega_c + \bar{\eta} \partial^2 & i\tilde{\omega} + \left(\eta + i \frac{s^2}{\omega}\right) \partial^2 \end{pmatrix} \mathbf{V} = -\frac{e\mathbf{E}_0}{m}, \quad (16)$$

where we introduce the simplified notations: $\partial = \partial/\partial y$, $\tilde{\omega} = \omega + i\gamma$, $\eta = \eta_{xx}(\omega)$, and $\bar{\eta} = \eta_{xy}(\omega)$. Equation (16) for the rough sample edges should be supplemented by the diffusive boundary conditions:

$$\mathbf{V}|_{y=\pm W/2} = 0. \quad (17)$$

We suppose that the rate of electron scattering on disorder, γ , is the smallest value among all other frequencies and rates of the problem: $\gamma \rightarrow 0$. The equation for the eigenvalues in this case is:

$$\begin{aligned} \left(i \frac{s^2}{\omega} \eta + \eta^2 + \bar{\eta}^2\right) \lambda^4 + (-s^2 + 2i\omega\eta + 2\omega_c\bar{\eta}) \lambda^2 + \\ + \omega_c^2 - \tilde{\omega}^2 = 0. \end{aligned} \quad (18)$$

The scattering rate γ should be kept only in the last term as the other terms have nonzero real as well as imaginary parts already at $\gamma = 0$.

The most transparent for analysis is the regime, when the spacescales corresponding to the two roots λ_1 and λ_2 of Eq. (18) have different orders of magnitudes: $|\text{Re}\lambda_1|, |\text{Im}\lambda_1| \ll |\text{Re}\lambda_2|, |\text{Im}\lambda_2|$. We will show below that this case is realized when

$$\frac{s}{v_F} \gg \omega\tau_{ee} \gg 1. \quad (19)$$

If this inequality is satisfied, calculations based on Eqs. (11) and (18) leads to:

$$\lambda_1^2 = \frac{\omega_c^2 - \tilde{\omega}^2}{s^2} (1 + iu), \quad \lambda_2^2 = -i \frac{\omega}{\eta} (1 - iw), \quad (20)$$

where the small parameters u and w , $|u|, |w| \ll 1$, are:

$$u = \frac{(\omega^2 + \omega_c^2)\eta - 2i\omega\omega_c\bar{\eta}}{\omega s^2}, \quad w = \frac{(\omega_c\eta - i\omega\bar{\eta})^2}{\omega\eta s^2}.$$

The first eigenvalue λ_1 describes the character length of the part of the response related to perturbation of charge, that is to magnetoplasmons. The corresponding to λ_1 damping coefficient $\Upsilon_p(q)$ outside the cyclotron resonance, $|\omega - \omega_c| \gg \gamma$, was calculated in Ref. [1]:

$$\Upsilon_p(q) = \frac{\omega_c^2 + \omega_p^2}{2\omega_p^2} q^2 \text{Re}\eta + \frac{\omega_c}{\omega_p} q^2 \text{Im}\bar{\eta}, \quad (21)$$

where the viscosity coefficients $\eta = \eta(\omega)$ and $\bar{\eta} = \bar{\eta}(\omega)$ are taken at the magnetoplasmon frequency $\omega = \omega_p(q)$.

Damping of magnetoplasmons due to scattering on disorder is important only in the vicinity of the cyclotron resonance, $|\omega - \omega_c| \lesssim \gamma$ [see Eq. (20)].

The second eigenvalue λ_2 corresponds to the standing waves of the transverse zero sound. Such waves exists in strongly non-ideal Fermi liquid at the frequencies $\omega \gg 1/\tau_{ee}$ [4]. They are similar to the transverse sound in highly viscous amorphous media, such as glasses, plastics, etc. The transverse zero sound is a characteristic phenomena to distinguish weakly (gas-like) and strongly (honey-like) viscous media: it is absent in the first and exist in the last. When the non-ideality of the Fermi liquid is very high, the longitudinal and the transverse zero sounds can be considered within hydrodynamics [5]. The electron-electron collisions, controlling relaxation of the viscous stress tensor, determine the damping coefficient of the transverse sound.

The dispersion law $\omega_s(q)$ and the damping coefficient $\Upsilon_s(q)$ of the transverse zero sound come from the second of Eq. (20):

$$\lambda_2^2 \approx -i \frac{\omega}{\eta(\omega, \omega_c)}, \quad (22)$$

if we put $\lambda_2 = iq$ (q is a real wavevector) and let ω have an imaginary part, proportional to the magnetosound damping coefficient Υ_s . At high frequencies, $\omega_c, \omega \gg 1/\tau_{ee}$, and far from the viscous resonance, $|\omega - 2\omega_c| \gg 1/\tau_{ee}$, we obtain from Eq. (20):

$$\omega_s(q) = \sqrt{4\omega_c^2 + \frac{v_F^2 q^2}{4}}, \quad \Upsilon_s(q) = \frac{4\omega_c^2 + \omega_s^2}{2\omega_s^2 \tau_{ee}}. \quad (23)$$

As we discussed above, for a strongly non-ideal Fermi liquid v_F is a parameter that enters in the zero-field viscosity coefficient as $\eta_0 = v_F^2 \tau_{ee}/4$ and is much greater than the actual Fermi velocity v_{F0} [5]. As a consequence, the minimal character length in the present theory, $l_\omega = v_F/\omega$, is much larger than the length of the path that a quasiparticle passes during one period of variation of ac field, $\sim v_{F0}/\omega$. Herewith we consider that $s \gg v_F$. Thus we are able to consider the flows $\mathbf{V}(y)$ having the character spacescales W as small as $v_{F0}/\omega \ll W \ll l_\omega$.

In Fig. 1(a) of the main text we have presented the dispersion laws of the magnetoplasmons and the transverse zero sound. In this work we do not study the detailed structure of waves near the interaction point of the magnetoplasmons and the transverse zero sound dispersion laws $\omega_p(q)$ and $\omega_s(q)$.

The straightforward calculations on base of Eqs. (16), (17), and (20) lead to the following result for the distribution of the velocity:

$$\mathbf{V}(y) = \frac{eE_0}{2m} [\mathbf{A}_0 + h(\lambda_1, y) \mathbf{A}_1 + h(\lambda_2, y) \mathbf{A}_2], \quad (24)$$

where

$$\mathbf{A}_0 = \frac{1}{\tilde{\omega} \pm \omega_c} \begin{pmatrix} i \\ \pm 1 \end{pmatrix}, \quad h(\lambda, y) = \frac{\cosh(\lambda y)}{\cosh(\lambda W/2)},$$

$$\mathbf{A}_1 = \pm \frac{1}{\omega(\bar{\omega} \pm \omega_c)} \begin{pmatrix} i\omega_c \\ -\omega \end{pmatrix} + \frac{\varepsilon}{\omega^2} \begin{pmatrix} -2\omega_c \pm \omega \\ -i\omega \end{pmatrix},$$

$$\mathbf{A}_2 = \frac{i}{\omega} \begin{pmatrix} -1 \\ \varepsilon \end{pmatrix} \left[1 + \frac{i\varepsilon}{\omega} (2\omega_c \mp \omega) \right],$$

and $\varepsilon = (\omega_c \eta - i\omega\bar{\eta})/s^2$.

It is seen from Eq. (24) that the viscoelastic part of the linear response is responsible for forming the flow in the very vicinities of the sample edges with the widths of the order of $L_s = 1/|\text{Re}\lambda_2|$ in the case $W \gg L_s$ [see Fig. 1(b) in the main text] or in the whole sample for very narrow samples, $W \ll L_s$. The plasmonic part of the linear response governs the flow in the wider near-edge layers with the widths of the order of $L_p = 1/|\text{Re}\lambda_1|$ in the very wide samples, $W \gg L_p$ [see Fig. 1(b) in the main text], or in the central part of the samples with the widths in the interval $L_s \ll W \ll L_p$. In the central part of the very wide samples, $W \gg L_p$, the flow is Ohmic: $\mathbf{V}(y) = eE_0\mathbf{A}_0/(2m)$ [see Fig. 1(b) in the main text]. It is controlled just by motion of individual electrons in external electric and magnetic fields and scattering on disorder.

For the complex amplitude

$$\mathbf{I} = en_0 \int_{-W/2}^{W/2} dy \mathbf{V}(y)$$

of the total electric current, $\mathbf{I}(t) = \mathbf{I}e^{-i\omega t} + c.c.$, we easily get from Eq. (24):

$$\mathbf{I} = \frac{e^2 n_0 E_0 W}{2m} [\mathbf{A}_0 + f(\lambda_1) \mathbf{A}_1 + f(\lambda_2) \mathbf{A}_2], \quad (25)$$

where

$$f(\lambda) = \frac{\tanh(\lambda W/2)}{\lambda W/2}.$$

Below in this section we perform analytical estimations of the eigenvalues λ_1 and λ_2 for the most interesting case of the large frequencies ω and ω_c having the same order of magnitude, being much greater than $1/\tau_{ee}$, and lying far or near the cyclotron and the viscous resonances.

For the frequencies ω above the cyclotron resonance, $\omega - \omega_c \gg \gamma$, the imaginary part of the plasmonic eigenvalue λ_1 is:

$$\text{Im } \lambda_1 \approx \frac{\sqrt{\omega^2 - \omega_c^2}}{s} \sim \frac{1}{l_p}. \quad (26)$$

Here and below we present, if it is possible, we present only the positive values of the imaginary and the real parts of the eigenvalues $\lambda_{1,2}$. The value of $\text{Im}\lambda_1$ in Eq. (26) is much greater than the real part λ_1 , which is:

$$\text{Re } \lambda_1 \approx \frac{1}{l_p s^2} \left(\frac{\omega^2 + \omega_c^2}{2\omega} \text{Re } \eta + \omega_c \text{Im } \bar{\eta} \right). \quad (27)$$

The last formula corresponds to the damping coefficient of magnetoplasmons due to viscosity (21). The values $\text{Re } \eta$ and $\text{Im } \bar{\eta}$, in their turn, strongly depend on the closeness of the frequencies ω and ω_c to the viscous resonance. For the frequencies far and in vicinity of the viscous resonance we obtain the two possible magnitudes of $\text{Re } \lambda_1$:

$$\text{Re } \lambda_1 \sim \frac{1}{l_p} \frac{v_F^2}{s^2} \begin{cases} 1/(\omega\tau_{ee}), & |\omega - 2\omega_c| \gg 1/\tau_{ee} \\ \omega\tau_{ee}, & |\omega - 2\omega_c| \lesssim 1/\tau_{ee} \end{cases}. \quad (28)$$

We see from Eqs. (26) and (28) that indeed $\text{Im } \lambda_1 \gg \text{Re } \lambda_1$, if the condition (19) is fulfilled.

Accordingly to Eqs. (26) and (28), above the cyclotron resonance the velocity profile $\mathbf{V}(y)$ is a standing magnetoplasmon wave with the wavelength $l_p \sim s/\omega$ and the length of decay $L_p^{\text{out}} \sim (s/v_F)^2 s\tau_{ee}$ outside the viscous resonance or $L_p^{\text{in}} \sim (s/v_F)^2 [s/(\omega^2\tau_{ee})]$ in the vicinity of the viscous resonance.

Below the cyclotron resonance, $\omega_c - \omega \gg \gamma$, the real part of the plasmonic eigenvalue λ_1 is much greater than its imaginary part:

$$\lambda_1 \approx \frac{\sqrt{\omega_c^2 - \omega^2}}{s} \sim \frac{1}{l_p}. \quad (29)$$

Thus the corresponding distribution of $\mathbf{V}(y)$ has the non-oscillating exponential profile with the character length $l_p = s/\omega$.

In the vicinity of the cyclotron resonance, $|\omega - \omega_c| \lesssim \gamma$, the real as well as the imaginary parts of the plasmonic eigenvalue are controlled by scattering on disorder:

$$\lambda_1 \approx \frac{\sqrt{\omega_c^2 - \omega^2 - 2i\gamma\omega}}{s}. \quad (30)$$

Such λ_1 corresponds to oscillations and exponential decay of $\mathbf{V}(y)$ with the same period and the decay length $\tilde{L}_p \sim s/\sqrt{\gamma\omega}$. At very weak scattering on disorder, $\gamma \rightarrow 0$, the lengthscale \tilde{L}_p is far greater than the lengths l_p , L_p^{in} and L_p^{out} of decay of the plasmonic contribution outside the cyclotron resonance.

The eigenvalue λ_2 depends only on the closeness of the frequencies ω and ω_c to the viscous resonance. Above the viscous resonance, $\omega - 2\omega_c \gg 1/\tau_{ee}$, we have:

$$\text{Im } \lambda_2 \approx \frac{2\sqrt{\omega^2 - 4\omega_c^2}}{v_F} \sim \frac{1}{l_{ee}} \quad (31)$$

and

$$\text{Re } \lambda_2 \approx \frac{2(4\omega_c^2 + \omega^2)}{v_F^2 \omega \tau_{ee} \text{Im } \lambda_2} \sim \frac{1}{l_{ee}}. \quad (32)$$

Here $l_{ee} = v_F \tau_{ee}$ is the parameter that is not the real scattering length of quasiparticles, but is the length-scale related with the viscosity coefficient η_0 as $l_{ee} = v_F \tau_{ee} 2\sqrt{\eta_0 \tau_{ee}}$, according to definition of v_F (see above).

We see that Eqs. (31) and (32) correspond to the dispersion law and the damping coefficient of the transverse zero sound (23). As $\text{Im} \lambda_2 \gg \text{Re} \lambda_2$, above the viscous resonance, $\omega - 2\omega_c \gg 1/\tau_{ee}$, the eigenvalue λ_2 corresponds to the standing waves of the transverse zero sound with the wavelength of the order of $l_s \equiv l_\omega$ and the length of decay $L_s \sim l_{ee}$.

Below the viscous resonance, $2\omega_c - \omega \ll 1/\tau_{ee}$, the eigenvalue λ_2 is mainly real:

$$\lambda_2 \approx \frac{2\sqrt{4\omega_c^2 - \omega^2}}{v_F} \sim \frac{1}{l_\omega}. \quad (33)$$

In this case the viscoelastic part of the response has the form of the exponential increase of $\mathbf{V}(y)$ from the edges into the bulk with the character length l_ω .

In the vicinity of the viscous resonance, $|\omega - 2\omega_c| \lesssim 1/\tau_{ee}$, we obtain from Eq. (20) the following result:

$$\lambda_2 \approx \frac{2\sqrt{4\omega_c^2 - \omega^2 - 4i\omega/\tau_{ee}}}{v_F}. \quad (34)$$

In this case, the eigenvalue λ_2 , as the eigenvalue λ_1 in Eq. (30) near the cyclotron resonance, corresponds to exponential decay and oscillations with the same character lengths $\sim \sqrt{l_\omega l_{ee}}$. The last value is much smaller than decay length, $L_s \sim l_{ee}$, of magnetosound above the viscous resonance and is much greater than the width of the near-edge regions, l_s , below the viscous resonance.

We see that the behavior of the eigenvalue λ_2 near and far from the viscous resonance is similar to the behavior of the eigenvalue λ_1 near and far from the cyclotron resonance.

As it is seen from Eqs. (26)-(32), the introduced above condition (19) guarantees that $L_p, l_p \gg L_s, l_s$. Thus the plasmonic and the viscoelastic parts of the linear response are located in the well-defined layers with the widths of the different orders of magnitude [see Fig. 1(b) of the main text].

An analytical calculation of $\mathbf{V}(y)$ in a general case when the condition (19) is failed and the character lengths of the plasmonic and the viscoelastic part of the linear response can intersect each other is very cumbersome. In this case, it is reasonable to use numerical calculations to obtain the resulting dependencies of $\mathbf{V}(y)$ and \mathbf{I} on ω and ω_c . However, as it is seen from Eq. (18), the values of $\mathbf{V}(y)$ and \mathbf{I} will still exhibit the cyclotron and the viscous resonances.

2. Analysis of the linear response

In this section we perform an analysis of the properties of the linear response of a 2D highly viscous electron fluid in a long sample.

The linear response $\mathbf{V}(y, t)$ calculated in the above section describes, in particular, absorption of energy from

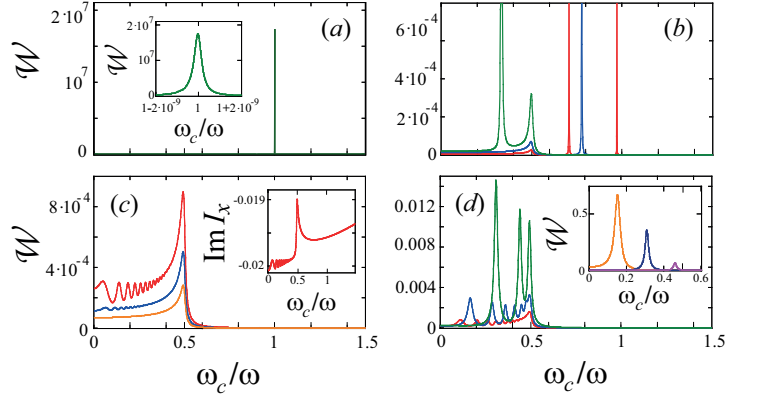


FIG. 4: The absorption power \mathcal{W} in units of $\mathcal{W}_0 = e^2 n_0 W E_0^2 \tau_{ee} / (2m)$ as a function of the cyclotron frequency ω_c at a fixed ac frequency ω for the very wide, wide, medium, and narrow samples. All curves are plotted for the following parameters: $\omega \tau_{ee} = 50$, $s/v_F = 300$, and $\gamma \tau_{ee} = 10^{-7}$. Panel (a) demonstrates $\mathcal{W}(\omega_c)$ for the very wide samples with $W/l_{ee} = 10^6$, that corresponds to $W/l_p \approx 2 \cdot 10^5$, $W/L_p^{out} \approx 0.04$, and $W/L_p^{in} \approx 10$. Panel (b) corresponds to the wide samples with $W/l_{ee} = 80, 30, 20$ (red, blue, and green curves); these values of W/l_{ee} correspond to $2\pi W/l_p \approx 5.0, 1.2, 0.9$. Panel (c) shows $\mathcal{W}(\omega_c)$ for the medium samples with $W/l_{ee} = 5.7, 3.2, 1.8$ and $W/l_\omega \approx 280, 160, 90$ (yellow, blue, and red curves). Panel (d) corresponds to the narrow samples with $W/l_{ee} = 1, 0.5, 0.2$ and $W/l_\omega = 50, 25, 10$ (red, blue, and green curves). Inset on panel (a) shows $\mathcal{W}(\omega_c)$ for the very wide sample with $W/l_{ee} = 10^6$ in large scale by the horizontal axis. Inset on panel (c) presents the imaginary part of the ac current $I_x(\omega_c)$ in units of $I_{x0} = e^2 n_0 W E_0 \tau_{ee} / (2m)$ for the case of the medium sample ($W/l_{ee} = 1.8$). Inset on panel (d) presents the absorption power $\mathcal{W}(\omega_c)$ in units of \mathcal{W}_0 for the very narrow samples ($W/l_{ee} = 0.08, 0.04, 0.033$ and $W/l_\omega \approx 0.4, 0.2, 0.16$ for purple, blue, and yellow curves); one can see disappearance of the last transverse sound resonances with decrease of W .

the ac external field $\mathbf{E}_0(t)$. The absorption power is:

$$\mathcal{W} = 2\text{Re}(\mathbf{E}_0^* \mathbf{I}) = E_0 \text{Re}(I_x \pm iI_y). \quad (35)$$

According to the above discussion, depending on the sample width W and the frequencies ω and ω_c , this value can be mainly determined by magnetoplasmons or by viscosity. We calculated the dependencies $\mathcal{W}(\omega_c)$ by Eqs. (25) and (35) at a fixed ac frequency ω for different sample widths W (see Fig. 4 and its descriptions below).

a) Wide samples: the behaviour of the plasmonic contribution.

In very wide samples:

$$W \gg L_p \gg l_p, \quad (36)$$

where $L_p = 1/\text{Re}\lambda_1$ and $l_p = s/\omega$, the plasmonic perturbation at the frequencies above the cyclotron resonance, $\omega - \omega_c \gg \gamma$, is formed in the near-edge regions with the widths of the order of L_p . The width L_p strongly depend on the closeness to the viscous resonance [see

Eq. (28)]. The viscoelastic perturbation is formed in the very vicinities of the edges with the widths of the order of $L_s = 1/\text{Re}\lambda_2$, $L_s \ll L_p$ [see Fig. 1(b) in the main text]. The contribution of the viscoelastic contribution to the current \mathbf{I} is negligibility small [see Eq. (24)]. In the central region, $W/2 - |y| \gtrsim \text{Re}\lambda_1$, the linear response is the Ohmic flow: it is formed just by the cyclotron motion of individual electrons and scattering on disorder. If the absorption power \mathcal{W} is mainly determined by the central region, the response exhibits the usual cyclotron resonance with a symmetric Lorentzian form exactly at $\omega = \omega_c$ [see Fig. 4(a)].

At the frequencies below the cyclotron resonance, $\omega_c - \omega \gg \gamma$, the plasmonic-like nonoscillating perturbation of the electron density and the hydrodynamic velocity are formed in the near-edge layers with the widths of the order of $l_p \sim s/\omega \ll L_p$. Near the cyclotron resonance, $|\omega - \omega_c| \lesssim \gamma$, the plasmonic perturbations have the character lengths, $\tilde{L}_p \sim s/\sqrt{\gamma\omega}$. As we have assumed that $\gamma \rightarrow 0$, this value can be greater than the sample width W .

In moderately wide samples:

$$l_p \ll W \ll L_p, \quad (37)$$

the plasmonic perturbations above the cyclotron resonance, $\omega - \omega_c \gg \gamma$, are formed inside the whole sample. When the sample width is equal to an integer or a half-integer number of the wavelengths of magnetoplasmons,

$$W = \frac{m\pi}{q_p(\omega, \omega_c)}, \quad (38)$$

the dependence $\mathcal{W}(\omega_c)$ exhibits the plasmonic resonances [see Fig. 4(b)]. In Eq. (38) m is an integer number and $q_p(\omega, \omega_c)$ is the root of Eq. (14). For a fixed ω the positions of the plasmonic resonance frequency $\omega_c^{p,m}(W)$ can fall in the vicinity of the viscous resonance frequency $\omega_c = \omega/2$. In this case, the half-width of the plasmonic resonance, which is proportional to the plasmon damping due to viscosity (21), resonantly depends on the difference $\omega_c - \omega/2$ [see Fig. 2(a) in the main text].

In moderately wide samples [Eq. (37)] the plasmonic part of the linear response below ($|\omega - \omega_c| \gg \gamma$) and near ($\omega_c - \omega \lesssim \gamma$) the cyclotron resonance has the same properties as in the very wide samples [Eq. (36)].

b) Narrow samples: the behavior of the viscoelastic contribution. In the samples of medium widths:

$$L_s \ll W \ll l_p, \quad (39)$$

where $L_s = 1/\text{Re}\lambda_2$, the viscoelastic part of the linear response, which is formed in the near-edge regions with the widths of the order of L_s , give a substantial contribution to the current $\mathbf{I}(t)$. In the central part of the sample, $W/2 - |y| \gg L_s$, the flow is still controlled by magnetoplasmons. The viscoelastic and the plasmonic contributions to the current can be comparable.

Above the viscous resonance, $\omega - 2\omega_c \gg 1/\tau_{ee}$ the flow in the near-edge regions, $W/2 - |y| \lesssim L_s$, have the form of standing waves of the transverse zero sound. Below the viscous resonance, $2\omega_c - \omega \gg 1/\tau_{ee}$, the viscoelastic part of the linear response is located in the narrower near-edge layers with the widths $\sim l_s \ll L_s$ and has the exponential non-oscillating profile. Due to the change of the character of the viscoelastic perturbation with the transition between these two regimes, the viscous resonance arises as a peak in the dependencies $\mathcal{W}(\omega_c)$ and $I_{x,y}(\omega_c)$ [see Fig. 4(c)]. From Eqs. (25) and (34) we immediately obtain for $\mathcal{W}(\omega_c)$ near the viscous resonance:

$$\mathcal{W}(\omega_c) \propto \text{Re} \left(\frac{1}{\sqrt{4\omega_c^2 - \omega^2 - 4i\omega/\tau_{ee}}} \right). \quad (40)$$

The peak (40) is strongly asymmetric relative to the point $\omega_c = \omega/2$.

Near the viscous resonance, $|\omega - 2\omega_c| \lesssim 1/\tau_{ee}$, the viscoelastic perturbation has the form of the oscillations near the sample edges rapidly decaying in the direction inside the bulk with the same period and the decay length given by Eq. (34).

In narrow samples,

$$l_s \ll W \ll L_s, \quad (41)$$

above the viscous resonance, $\omega - 2\omega_c \gg 1/\tau_{ee}$ the flow is controlled by viscosity in the whole sample. The distribution of the hydrodynamic velocity have the form of standing waves of the transverse zero sound. When the sample width becomes equal to an integer or a half-integer number of wavelengths of the transverse sound,

$$W = \frac{m\pi}{q_s(\omega, \omega_c)}, \quad (42)$$

the resonances related to forming of the standing waves of the transverse sound occurs above the viscous resonance and exhibit themselves in $\mathcal{W}(\omega_c)$ [see Figs. 4(c,d)]. In Eq. (42) m is an integer number and $q_s(\omega, \omega_c)$ is the root of Eq. (23). Such resonances are similar to the plasmonic resonances and the resonances of any standing waves in a resonator. They can be named “the transverse zero sound resonances” or “magneto-sound resonances”.

In narrow samples [Eq. (41)] below the viscous resonance, $2\omega_c - \omega \gg 1/\tau_{ee}$, the viscoelastic part of the flow is non-oscillating exponential growth in the directions from the edges into the bulk and is located in the near-edge regions with the widths of the order of l_s (similarly as in medium samples).

In maximally narrow samples,

$$W \ll l_s, \quad (43)$$

the viscoelastic contribution also dominates. The flow has a parabolic profile in the whole sample [see Eq. (24) in the limit $\lambda_{1,2} \rightarrow 0$]. This regime can be regarded as

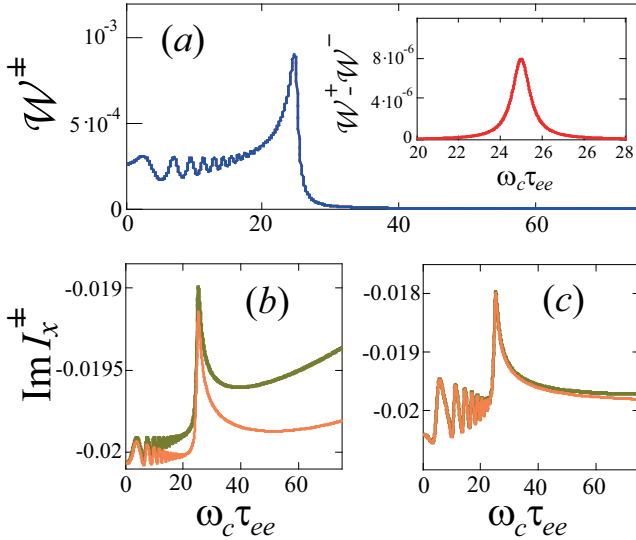


FIG. 5: Panel (a) shows the absorption power $W^\pm(\omega_c) \approx E_0 \text{Re} I_x^\pm(\omega_c)$ in units of W_0 for the case of the medium sample width ($W/l_{ee} = 1.8$) for the right (+) and left (-) polarizations of the ac fields. Inset on panel (a) shows the difference $W^+(\omega_c) - W^-(\omega_c)$ near the plasmonic resonance, $\omega_c = \omega/2$. It is seen that the dependencies for the both polarizations almost coincide. The parameters of the system are the same as in Fig. 4: $\omega\tau_{ee} = 50$, $s/v_F = 300$, and $\gamma\tau_{ee} = 10^{-7}$. Panels (b) and (c) demonstrates the imaginary part of the ac current, $\text{Im} I_x^\pm(\omega_c)$, in units of I_{x0} for the medium sample widths [$W/l_{ee} = 1.8$ for panel (b) and $W/l_{ee} = 0.8$ for panel (c)]. Orange and green curves correspond to the right and left polarizations.

the ac Poiseuille flow in magnetic field. For the current we obtain from (25):

$$I_x = \frac{e^2 n_0 E_0 W^3}{24 m \eta_0} \frac{\omega^2 + 4\omega_c^2 + i\omega\tau_{ee}(-\omega^2 + 4\omega_c^2)}{\omega^2} \quad (44)$$

and $|I_y| \ll |I_x|$. We see from Eq. (44) that the viscous resonance manifests itself not in the current, but in the ac impedance $Z = E/I_x$. Near the resonance we have from Eq. (44):

$$\text{Re} Z \propto \frac{1}{1 + (\omega - 2\omega_c)^2 \tau_{ee}^2}. \quad (45)$$

In the limit $\omega\tau_{ee} \gg 1$ the imaginary part of the current (44) is independent on any relaxation parameter. The motion of the fluid in this regime resembles oscillations of a charged elastic media, glued near at the edges $y = \pm W/2$, in response of ac external field. Herewith the real part of Eq. (44) describes the relaxation of such elastic oscillations. By this way, for the maximally narrow samples, $v_{F0}/\omega \ll W \ll l_\omega$, the viscoelasticity transition occurs at $\omega\tau_{ee} \sim 1$.

By this way, the viscous resonance manifests itself in different ways depending on the sample width W . In wide samples it can be observed by the resonant dependence

of the half-width of the plasmonic resonance on W . In medium samples, if the main contribution to the linear response comes from the viscoelastic part of the flow, the viscous resonance occurs due to changing of the character of the viscoelastic part of the flow, which is standing magnetosonic waves at the ac frequencies above the viscous resonance and a non-oscillating decay below the viscous resonance. In this case, the dependence $W(\omega_c)$ has the form of an asymmetrical peak near $\omega = 2\omega_c$. In narrow samples when the standing waves of zero sound are well-formed, the magnetosound resonances related to coincidence of the sample width with an integer or half-integer number of wavelengths of the transverse sound, appear in the dependence $W(\omega_c)$. In narrowest samples the ac Poiseuille flow is formed and the viscous resonance manifest itself in the sample impedance.

An important feature of the viscoelastic part of the linear response is its independence on the sign of the circular polarization of ac field [see Eq. (24)]. With decrease the sample width, the dependence of I and W on the sign of the circular polarization becomes weaker and, finally, almost vanish for for both real and imaginary parts at the sample widths W of the order of the decay length of magnetosound, $L_s \sim l_{ee}$ (see Fig. 5). Herewith this dependence disappears faster for the real part of the current I_x , than for its imaginary part than.

3. Experimental results on non-linear ac effects in high-mobility GaAs quantum wells and possible hydrodynamic description of these effects

It seems very possible that the viscous resonance is responsible for the giant peak in photoresistance [6, 7] and the peculiarities the photovoltaic effect [8], that were observed at $\omega = 2\omega_c$ in the high-mobility GaAs quantum wells.

Indeed, first, it was stressed in Ref. [6] that the peak in photoresistance and a very well pronounced giant negative magnetoresistance, explained in Ref. [9] as a manifestation of forming of a viscous flow, are observed in the *same best-quality* GaAs structures. If 2D electrons in such structures form a viscous fluid, then any response of the system on ac field (absorption, photovoltage, photoresistance) must inevitably have peculiarities at the frequency of the viscous resonance.

Second, in the current paper we demonstrated that the peak of the viscous resonance can be asymmetric as well as symmetric, depending on the sample width. Both these two forms of the peak are observed in the experiments [6, 7] in different samples at different conditions.

Third, in Ref. [8] numerous magnetoplasmon resonances were observed in the photovoltage signal on several GaAs high-quality structures of different geometries. The peculiarity at $\omega = 2\omega_c$ on the background of the “forest” of plasmonic resonances was seen in the meander-

gated samples. In such structures the space inhomogeneity of the flow and the relative role of viscosity are expected to be greater, compared with the other studied samples with flat gates and without any gates, where a smeared peculiarity and no peculiarity was observed at $\omega = 2\omega_c$.

Beside this, the following circumstances should be noted. It was experimentally shown in Refs. [10, 11] that photoresistance and, in particular, the micro-wave induced resistance oscillations (MIRO) in high-mobility GaAs quantum wells do not depend on the sign of circular polarization of radiation at $\omega_c \lesssim \omega$. At the same time, moderate negative magnetoresistance at low temperatures was observed [11] on the sample studied in Ref. [10, 11] (at higher temperatures a positive magnetoresistance was observed). With increase of the frequency, the profile of the MIRO oscillations in the region $\omega_c \approx \omega/2$ becomes more irregular (not sinusoidal) and exhibits some peak near $\omega_c \approx \omega/2$, as it was also observed in a more pronounced manner in Ref. [7].

By this way, in Refs. [10, 11] a correlation between the appearance of a peak-like feature in photoconductivity near $\omega_c \approx \omega/2$ and the independence of photoresistance on the sign of the circular polarization was, possibly, established. In the current paper we demonstrate that the viscoelastic part of the linear response is independent on the sign of the circular polarization. These facts could be an additional evidence that the peak at $\omega = 2\omega_c$ in photoresistance of the high-mobility GaAs quantum wells is related to the viscous resonance.

Oscillations of photoresistance of high-quality GaAs quantum wells were recently observed for the case of radiation in the terahertz diapason [12, 13]. The properties of the revealed oscillations are very similar to those of MIRO, in particular, they weakly depend or almost do not depend on the sign of the circular polarization of radiation.

The assumption about a strong interaction between quasiparticles in the 2D electron Fermi liquid in the high-mobility GaAs quantum wells seems to be fulfilled because of the two following facts. First, the parameter r_s that characterize the strengths of the Coulomb interaction in a 2D electron system is about unity for the structures studied in Refs. [6–8]. Second, there are the experimental evidences that the effective mass of 2D electrons in high-mobility GaAs quantum wells is strongly renormalized due to inter-particle interaction [14, 15]. A preliminary analysis [5] demonstrates that a strong interaction between quasiparticles of the 2D electron Fermi liquid justify the applicability of hydrodynamics for the proper description of such highly viscous fluids at the frequencies $\omega \gg 1/\tau_{ee}$.

To construct the theories of the photoresistance and the photovoltaic effects, one should take into account some nonlinear terms in the hydrodynamic equation (10) following, for example, Refs. [16, 17]. In these works the

theories of the photovoltaic effect and the MIRO oscillations in photoresistance were developed for 2D electrons in a disordered systems. One of the main elements of the theories [16, 17] is the linear response of free 2D electrons on ac field: $\mathbf{V}_0(y) = eE_0\mathbf{A}_0/(2m)$. In the theory of the photoresistance and the photovoltage effects in a viscous electron fluid in a sample without disorder, the linear response (24) should be used instead of $\mathbf{V}_0(y)$.

All the previous theories of the MIRO effect were developed for the model of 2D electrons in a disordered system [18]. These theories explained very well the shape of photoresistance oscillations and their dependence on temperature and other parameters. The main problem of all the theories was the inconsistency between the lack of dependence of the effect on the sign of the circular polarization in experiment and the presence of such a dependence in theories. As we now have the evidences that 2D electrons in high-mobility GaAs structures form a highly viscous fluid (“electron honey”), it is logical to construct the theory of the MIRO effect for the case of such fluid flowing in a sample without any disorder.

In real samples, apparently, there exist the two contributions to photoresistance and other kinetic effects: the part of the signal is controlled by scattering of individual electrons on disorder and the other part is controlled by forming the electron fluid, being is independent on the sign of the circular polarization.

The theory [17] takes into account the memory effects in scattering of electrons on smooth localized defects in magnetic field. This lead to a proper description of the MIRO oscillations except the explanation of their independence the sign of the circular polarization. Possibly, taking into account the memory effects in *electron-electron scattering* in the hydrodynamic theory of non-linear magnetotransport will lead not only to explanation of the giant peak in photoresistance, but also to a proper description of the MIRO oscillations, similar to the description within the models for 2D independent electrons in samples with bulk disorder. The memory effects in interparticle collisions were considered for the case of Boltzmann gas in Refs. [19, 20] and, very recently, for hydrodynamic transport of electrons in graphene in Ref. [21]. In the future possible theory of hydrodynamic magnetotransport taking into account the memory effects in electron-electron collisions in magnetic field, the calculated linear response (24) will be an element, which will be used instead of the linear response of free electrons. Thus the resulting photoresistance at magnetic fields $\omega_c < \omega$ will not depend on the sign of the circular polarization for the narrow samples.

[1] P. S. Alekseev, Phys. Rev. B 98, 165440 (2018).

[2] V. I. Fal’ko and D. E. Khmel’nitskii, JETP 68, 1150

- (1989).
- [3] V. A. Volkov and A. A. Zabolotnykh, *Phys. Rev. B* 89, 121410 (2014).
 - [4] E. M. Lifshitz, L. P. Pitaevskii, *Statistical Physics, Part 2: Theory of the Condensed State. Vol. 9 (1st ed.)*. Pergamon Press (1981).
 - [5] P. S. Alekseev and A. P. Alekseeva, to be published.
 - [6] Y. Dai, R. R. Du, L. N. Pfeiffer, and K. W. West, *Phys. Rev. Lett.* 105, 246802 (2010).
 - [7] A. T. Hatke, M. A. Zudov, L. N. Pfeiffer, and K. W. West, *Phys. Rev B* 84, 241304 (2011).
 - [8] M. Bialek, J. Lusakowski, M. Czapkiewicz, J. Wrobel, and V. Umansky, *Phys. Rev B* 91, 045437 (2015).
 - [9] P. S. Alekseev, *Phys. Rev. Lett.* 117, 166601 (2016).
 - [10] J. H. Smet, B. Gorshunov, C. Jiang, L. Pfeiffer, K. West, V. Umansky, M. Dressel, R. Meisels, F. Kuchar, and K. von Klitzing *Phys. Rev. Lett.* 95, 116804 (2007).
 - [11] J.H. Smet, B. Gorshunov, C. Jiang, L. Pfeiffer, K. West, V. Umansky, M. Dressel, R. Meisels, F. Kuchar, K. von Klitzing, *Physica E* 35, 315 (2006).
 - [12] T. Herrmann, I. A. Dmitriev, D. A. Kozlov, M. Schneider, B. Jentzsch, Z. D. Kvon, P. Olbrich, V. V. Belkov, A. Bayer, D. Schuh, D. Bougeard, T. Kuczmik, M. Oltcher, D. Weiss, and S. D. Ganichev *Phys. Rev. B* 94, 081301 (2016).
 - [13] T. Herrmann, Z. D. Kvon, I. A. Dmitriev, D. A. Kozlov, B. Jentzsch, M. Schneider, L. Schell, V. V. Belkov, A. Bayer, D. Schuh, D. Bougeard, T. Kuczmik, M. Oltcher, D. Weiss, and S. D. Ganichev, *Phys. Rev. B* 96, 115449 (2017).
 - [14] I. V. Kukushkin and V. A. Volkov, Two-dimensional electronic fluid in strong magnetic field, (Moscow, Fizmatkniga, 2016).
 - [15] A. V. Shchepetilnikov, D. D. Frolov, Yu. A. Nefyodov, I. V. Kukushkin, and S. Schmult *Phys. Rev. B* 95, 161305 (2017).
 - [16] M. B. Lifshits and M. I. Dyakonov, *Phys. Rev. B* 80, 121304 (2009).
 - [17] Y. M. Beltukov and M. I. Dyakonov, *Phys. Rev. Lett.* 116, 176801 (2016).
 - [18] I. A. Dmitriev, A. D. Mirlin, D. G. Polyakov, and M. A. Zudov, *Rev. Mod. Phys.* 84, 1709 (2012).
 - [19] J. R. Dorfman and E. G. D. Cohen, *Phys. Lett.* 66, 124 (1965)
 - [20] J. R. Dorfman and E. G. D. Cohen, *Phys. Rev. Lett.* 25, 1257 (1970).
 - [21] A. Shytov, J. Feng Kong, G. Falkovich, and L. Levitov, *Phys. Rev. Lett.* 121, 176805 (2018).